Trop J Nat Prod Res, September 2024; 8(9): 8400-8411 **ISSN 2616-0684 (Print)**
ISSN 2616-0692 (Electronic)

Tropical Journal of Natural Product Research

Available online at https://www.tjnpr.org

Original Research Article

In vitro and Molecular Docking Evaluation of the Antibacterial, Antioxidant, and Antidiabetic Effects of Silver Nanoparticles from *Cymbopogon citratus* Leaf

Olasunkanmi K. Awote[1]*, Kehinde O. Amisu[2], Olajide S. Anagun[2], Fifame P. Dohou[1], Eniola R. Olokunola[1], Nzubechi O. Elum[1]

[1]*Department of Biochemistry, Faculty of Science, Lagos State University, Ojo, Nigeria*
[2]*Department of Microbiology, Faculty of Science, Lagos State University, Ojo, Nigeria*

ARTICLE INFO

Article history:
Received: 05 July 2024
Revised: 12 August 2024
Accepted: 15 September 2024
Published online: 01 October 2024

ABSTRACT

Diabetes and multidrug-resistant (MDR) bacterial infections remain very common worldwide. This study investigated the antioxidant, antibacterial, and antidiabetic potentials of silver nanoparticles (AgNPs) from *Cymbopogon citratus* aqueous leaf extract (CCALE). AgNPs were synthesized in a 9:1 of 1 mM $AgNO_3$ solution to CCALE. The synthesis was monitored *via* colour change and UV-visible spectrophotometry and later characterized using Fourier transform infrared spectroscopy (FTIR), energy dispersive x-ray (EDX), transmission electron microscopy (TEM), X-ray diffraction (XRD), and thermogravimetric analysis (TGA). Using standard procedures, gas chromatography-mass spectrometry (GC-MS) and antioxidant assays (reducing power, ferric reducing antioxidant power, total antioxidant capacity, and DPPH radical scavenging) of AgNPs were performed. Antibacterial activities against MDR bacterial isolates were assessed using the agar-diffusion method. Molecular docking studies were conducted using PyRx and Biovia Discovery Studio with 3D conformers of CCALE phyto-compounds retrieved from PubChem and 11-β-hydroxysteroid and Vaspin proteins from the RCSB Protein Data Bank. The AgNPs showed a light brown colour and a UV-Vis absorption peak at 445 nm. TEM revealed spherical particles (9.22 to 12.54 nm). EDX confirmed significant silver content. FTIR indicated the presence of alkynes, carboxylic acids, and alcohol groups. XRD showed diffraction peaks at $2\theta = 38°$, 44.5°, and 64.5°, corresponding to the (111), (200), and (220) reflection planes. TGA indicated volatility and thermal stability. The AgNPs demonstrated strong antioxidant and antibacterial activities, particularly against *Klebsiella pneumoniae*, *Salmonella typhi*, and *Staphylococcus aureus*. Stigmasterol exhibited the best binding affinity with the protein targets, suggesting CCALE-AgNPs as a potential antioxidant, antibacterial, and antidiabetic drug candidate.

Keywords: Diabetes mellitus, Antioxidant, *Cymbopogon citratus* Leaf, Silver nanoparticles, Multi-drug resistance, Antibacterial, Molecular docking.

Introduction

Nanotechnology is a field of science and engineering concerned with creating and applying structures and systems to manipulate atoms and molecules at the nano-scales (1 - 100 nm).[1] Due to a unique nano-structure and size feature, nanoparticles (NPs) have been considered important in the drug delivery systems field for the treatment of various diseases including diabetes and infectious diseases.[2,3] NPs are also used for catalysis, composite materials such as polymer preparations, sensor technology, food and agriculture, and optoelectronic recorded media labeling.[4] NP synthesis can either be via physical, chemical, or biological methods. However, b-oth the physical and chemical methods have recently faced various limitations including their harmful effect on living organisms, expensive methods of synthesis, tedious processes, and hazardous chemical generation.[5]

*Corresponding author. Email: olasunkanmi.awote@lasu.edu.ng
Tel: +234-8088840835.

Citation: Awote OK, Amisu KO, Anagun OS, Dohou FP, Olokunola ER, ElumNO. *In vitro* and Molecular Docking Evaluation of the Antibacterial, Antioxidant, and Antidiabetic Effects of Silver Nanoparticles from *Cymbopogon citratus* Leaf. Trop J Nat Prod Res. 2024; 8(9): 8400 – 8411. https://doi.org/10.26538/tjnpr/v8i9.23

Official Journal of Natural Product Research Group, Faculty of Pharmacy, University of Benin, Benin City, Nigeria

Biological synthesis involving either the use of medicinal plants (green synthesis), micro-organisms, yeast, algae, or fungi, has gained better attention because of its low cost, easy process, and less harm.[6]Silver nanoparticles (AgNPs), have proven to be one of the most appealing nano-materials in biomedicine and are well-known for their potent, broad-spectrum antibacterial, anti-inflammatory, and anticancer properties, in addition to other associated biological functions.[7,8]Diabetes mellitus (DM) is a complex metabolic disorder identified by persistent hyperglycemia resulting from gross disorganization of carbohydrate, fat, and protein metabolism due to insulin insufficiency or deficiency.[5] Individuals with diabetes usually have an impaired immune system, making them more susceptible to infections and requiring frequent, prolonged antibiotic use for conditions such as urinary tract infections, foot infections, and respiratory infections. Thus, the effective management of DM and careful antibiotic use are critical in addressing the challenges posed by MDR infections in diabetic conditions. Furthermore, the generation of free radicals in diabetes leads to oxidative stress (an imbalance between free radicals and antioxidants), which exacerbates cellular damage and contributes to the progression of diabetic complications. In this case, antioxidants play a crucial role in neutralizing these generated free radicals, thereby mitigating oxidative damage and improving metabolic control in diabetic patients.[5]Natural products, especially medicinal plants are the primary source of drug candidates.[9] Moreso, plant-based preparations are the mainstay of all current medicines, particularly in rural regions due to their ease of availability, low cost, and little or no adverse effects.[10] Additionally, a variety of plants are a rich source of bioactive compounds, which have potent pharmacological benefits such as anti-inflammatory, anti-diabetic, and antioxidant properties without causing negative side effects.[11] More than 80% of people in Africa live

in low-resource environments and rely on medicinal plants to cure one illness or the other, including diabetes mellitus. Africa has an abundance of medicinal plants, many of which are utilized locally to cure a variety of ailments and diseases.[12]*Cymbopogon citratus* (Poaceae family), commonly called "lemongrass," is a valuable dietary and therapeutic herb, in most tropical regions. [13,14] Lemongrass is not only known for its pleasant citrus flavor and aromatic essence but also for a myriad of biological activities including anti-inflammatory, anti-nociceptive, antioxidant, anti-diabetic, antimicrobial, and anticancer properties, etc.[13-18]Several bioactive compounds, including luteolin, quercetin, kaempferol, and apigenin, as well as essential oils such as citral, borneol, geraniol, beta-myrcene, pinene, and farnesol, have been associated with these biological activities.[19-21] Therefore, based on the aforementioned individual biological attributes of *C. citratus* leaf and silver nanoparticles, this study aimed to explore the synthesis of silver nanoparticles using *Cymbopogon citratus* aqueous leaf extract (CCALE) and investigate its effects on generated free radicals, bacteria, and diabetes using *in vitro* and *in silico* methodologies.

Materials and Methods

Plant collection and identification

Fresh leaves of *Cymbopogon citratus* were harvested from Aiyetoro (latitude: 70 12' N and 30 3' E), Itele, Ogun State, Nigeria, on August 2023. The plant was identified and authenticated by a botanist, Dr. O. K. Oluwa in the herbarium of the Department of Botany, Faculty of Science, Lagos State University, Ojo, Nigeria, and issued a voucher number of LSH001092.

Plant extraction process

Cymbopogon citratus leaf was washed several times with clean water and later with deionized water and allowed to dry for a few minutes on the laboratory table. The cleaned fresh plant leaves were blended separately into possible smaller forms with a Scanfrost blender (model No: SFKAB409), and a 10% (w/v) aqueous extract of *Cymbopogon citratus* leaf was prepared and filtered twice using Whatman filter paper grade 1. The resulting extracts were then stored in the laboratory refrigerator for further use.[5]

Synthesis of Silver nanoparticles (AgNPs)

Silver nanoparticles (1:9 w/v) were synthesized by mixing 90 mL of silver nitrate solution (1mM $AgNO_3$ (Molychem, India) with 10 mL of CCALE. Two (2) mL aliquots of the synthesized AgNPs were taken after one hour to five hours of AgNPs synthesis, and the absorbance was analyzed (200-700 nm) with a UV-visible spectrophotometer (model No: Beckman DU640).[22]

Phytochemical screening of CCALE and its synthesized AgNPs

Polyphenolic constituents of the aqueous extracts of *Cymbopogon citratus* leaf *and its synthesized AgNPs*were quantified using the standard procedures and methods described by Awote *et al*.[5,22]

Gas chromatography-mass spectroscopy (GCMS) Analysis of CCALE

GC-MS analysis of the extract was performed using an Agilent 5977B GC/MSD system coupled with Agilent 8860 auto-sampler, a gas chromatograph interfaced to a mass spectrometer (GC-MS) equipped with an Elite-5MS (5% diphenyl/95% dimethyl polysiloxane) fused a capillary column (30 × 0.25µm ID × 0.25 µmdf). For GC-MS detection, an electron ionization system was operated in electron impact mode with an ionization energy of 70 eV. Helium gas (99.999%) was used as a carrier gas at a constant flow rate of 1 mL/min, and an injection volume of 1µL was employed (a split ratio of 10:1). Five (5) point serial dilution calibration standards (1.25, 2.5, 5.0, and 10.0 ppm) were prepared from the stock solution of 40 ppm and used to calibrate the GC-MS. The injector temperature was maintained at 300°C, the ion-source temperature was 250°C, and the oven temperature was programmed from 100°C (isothermal for 0.5 min) with an increase of 20 °C/min to 280 °C (2.5 min), Mass spectra were taken at 70 eV; a scanning interval of 0.5 s and fragments from 45 to 450 Da. The solvent delay was 0 to 3 min, and the total GC/MS running time was 21.33 min. [23]

Characterization of synthesized AgNPs

The synthesized AgNPs were further confirmed with UV-visible spectroscopy to determine if the AgNPs were within the range of silver nanoparticles synthesis. The elemental composition of AgNPs was assessed via an energy-dispersive x-ray (EDX) spectrophotometer (Oxford, UK).[24] FTIR (Fourier Transform Infra-Red) spectroscopy was achieved with an Alpha FTIR coupled with a platinum ATR (Bruker, USA) (FTIR). The film developed was used for the measurement of the spectra by scanning between 400 and 4000 cm^{-1}.[25] The crystalline phase of the AgNPs was identified using an XRD D8 Advanced diffractometer (Bruker, USA). The diffractogram was run from 20 to 90° of the Bragge angle 2θ at an increment of 0.01 and a scan speed of 0.2.[24] The average diameter of the synthesized AgNPs was conducted using a transmission electron microscope (JEOL TEM 2010, USA) and interpreted with ImageJ software.[26]The thermogravimetric analysis (TGA) of nanoparticles was conducted in a nitrogen atmosphere on a Seiko EXSTAR 6000 thermal analyzer at a scanning rate of 10 °C/min.[27]

Determination of Antioxidant Activity

2,2-diphenyl-1-picrylhydrazyl (DPPH)Scavenging Activity

The extract and the synthesized AgNPs (0.2 mL) each were mixed with 2 mL of 0.5 mM DPPH (Sigma Aldrich, USA) solution and incubated for 30 min at room temperature. Absorbance was measured by using a UV-Vis spectrophotometer (UV-VIS 1700, Shimadzu) at 517 nm. The percentage inhibition of the DPPH radical was calculated

$$\text{Using } \%\ DPPH\ Inhibition = \left(\frac{[\text{Abr} - \text{Aar}]}{\text{Abr}}\right) \text{X } 100 \ldots\ldots\ldots (1)$$

Where A_{br} is the absorbance before the reaction and A_{ar} is the absorbance after the reaction.[5,22]

Reducing power

The extract and the synthesized AgNPs (1 mL) each were mixed with 2.5 mL of 0.2 M phosphate buffer (pH 6.6) and 2.5 mL of 1% $K_3Fe(CN)_6$ (Molychem, India), then incubated at 50 °C for 20 min. After adding 2.5 mL of 10% trichloroacetic acid (Sigma Aldrich, USA), the mixture was centrifuged at 3000 rpm for 10 minutes. The supernatant (2.5 mL) was mixed with 2.5 mL of distilled water and 0.5 mL of 0.1% $FeCl_3$,and absorbance was measured by using a UV-vis spectrophotometer (UV-VIS 1700, Shimadzu) at 700 nm. [5,22]

Total Antioxidant Capacity (TAC)

The total antioxidant capacity was determined by mixing a 25 µL aliquot of the extract and the synthesized AgNPs each with 300 µL of TAC reagent, incubating for 90 minutes, and measuring absorbance with a UV-vis spectrophotometer (UV-VIS 1700, Shimadzu) at 630 nm. The percentage of total antioxidant capacity of CC-AgNPs was calculated using $\%\ TAC = \left(\frac{[\text{Abr} - \text{Aar}]}{\text{Abr}}\right) \text{X } 100 \ldots\ldots\ldots (2)$ and expressed as a percentage (%) of ascorbic acid [5,22] where A_{br} is the absorbance before the reaction and A_{ar} is the absorbance after the reaction.

Ferric reducing antioxidant power (FRAP)

The preparation of the FRAP reagent was done by using acetate buffer (pH 3.6), 10 mM of 2,4,6-tripyridyl-s-triazine (TPTZ) (Sigma Aldrich, USA) solution in 40 mM HCl, and 20 mM ferric chloride (Molychem, India) solution in the ratio of 10:1:1 (volume/volume), respectively. The freshly prepared FRAP reagent was warmed to 38 °C, and a total of 0.5 mL of each of the extract and synthesized AgNPs were mixed with 4 mL of FRAP reagent. The absorbance of the mixture was measured by using a UV-Vis spectrophotometer (UV-VIS 1700, Shimadzu) at 593 nm. The standard curve for ascorbic acid was made using the same method. The results are shown as mg ascorbic acid/g of extract sample. [5,22]

Determination of Antimicrobial Activity

Bacterial Culture Collection

Clinically important micro-organisms, including *Pseudomonas aeruginosa, Klebsiella pneumoniae, Escherichia coli, Staphylococcus aureus, Salmonella typhi*, and *Proteus mirabilis*, were obtained from the Microbiology Department's culture repository at Lagos State University (LASU). These pure cultures were sub-cultured on nutrient agar slants and stored at room temperature (27°C) until further use.

Antibacterial activity (agar diffusion method)

Briefly, pure colonies were picked using a sterile loop, emulsified in 10 mL of normal saline, and swabbed onto Mueller-Hinton agar plates. After drying for 5 min, wells were created with a 9 mm-sized sterile cork borer and filled with 100 µL of the extract and AgNPs using a micropipette. Plates were later incubated at 37°C for 24 hr, and the diameter of inhibition zones was measured in millimeters (mm).[28]

In-silico antidiabetic potential (Molecular docking method)
Protein preparation
The crystal structures of 11*β*-hydroxysteroid dehydrogenase and Vaspin were retrieved in .pdb format from the Protein Data Bank (PDB). For this study, a single protein chain was used for the docking analysis, while Biovia software was used to add polar hydrogens and also delete water molecules and co-crystallized ligands to prepare the proteins.[23]

Ligand preparation and docking protocol
The 3D crystal structures of the secondary metabolites (ligands) from GC-MS analysis were obtained from PubChem in .sdf format and converted to .pdb and .mol formats using Biovia Discovery Studio 2021. Canonical SMILES of each ligand were also retrieved from PubChem. Ligand energies were minimized using the Open Babel MMFF94 force field, and the minimized ligands were converted to .pdbqt format for AutoDock. Molecular docking studies were conducted using PyRx, based on binding free energy values. Ligand molecules were sorted by increasing docking energies. Protein-ligand interactions for the docked poses were analyzed at the binding sites of the target proteins.[23] Direct inhibitors of vaspinare not well-documented. Instead, the regulation of vaspin expression is more commonly studied as done in this study. Conversely, carbenoxolone was incorporated as the standard/ known inhibitor for 11β-hydroxysteroid dehydrogenase.

Chemical absorption, distribution, metabolism, excretion, and toxicity (ADMET) profiling
The physicochemical, pharmacokinetic, medicinal chemistry, lipophilicity, water solubility, and drug-likeness profile of the overall top binding ligands (candidate drugs) were predicted using SwissADME and admetSAR.[23]

Statistical analysis
The results were presented as Mean ± SEM (standard error of means). One-way analysis of variance (ANOVA) at a 95% confidence interval in GraphPad Prism software version 5.0 (San Diego, CA, USA) was used to determine statistically significant differences between the compared groups at $p < 0.05$.

Results and Discussion

The synthesis of silver nanoparticles was confirmed firstly by the change in color to brown (Figure 1a), however, further confirmation was performed using UV-visible spectral analysis monitored between 200 – 700nm. The maximum absorbance peak of the synthesized AgNPs was obtained at 445 nm (Figure 1b), which is within the range of silver nanoparticles.[29]

The EDX and TEM results showed the elemental composition, and internal nano-structures of the synthesized AgNPs, respectively. The atomic and weight concentrations of the embedded elemental composition include silver (17.53, 44.93), magnesium (42.27, 24.42), silicon (9.93, 6.63), sodium (9.37, 5.12), potassium (5.00, 4.65), chlorine (5.30, 4.47), calcium (3.57, 3.40), sulfur (2.65, 2.02), phosphorus (2.06, 1.51), iron (1.13, 1.50) and Titanium (1.19, 1.35), respectively (Figure 2a). This elemental profile showed a higher count at 1.5 keV due to the silver, thus further confirming the formation of silver nanoparticles. EDX analysis gives a qualitative as well as quantitative status of the elements that may be involved in the formation of nanoparticles.[30] The TEM image showed a spherical well-dispersed nanoparticle with low agglomeration and a size range between 9.22 and 12.54 nm (Figure 2b). This may confer their ability to penetrate cells/microbes and perform biological functions including antibacterial, antioxidant, antiglycation, anti-inflammatory, and antidiabetic properties.[30]

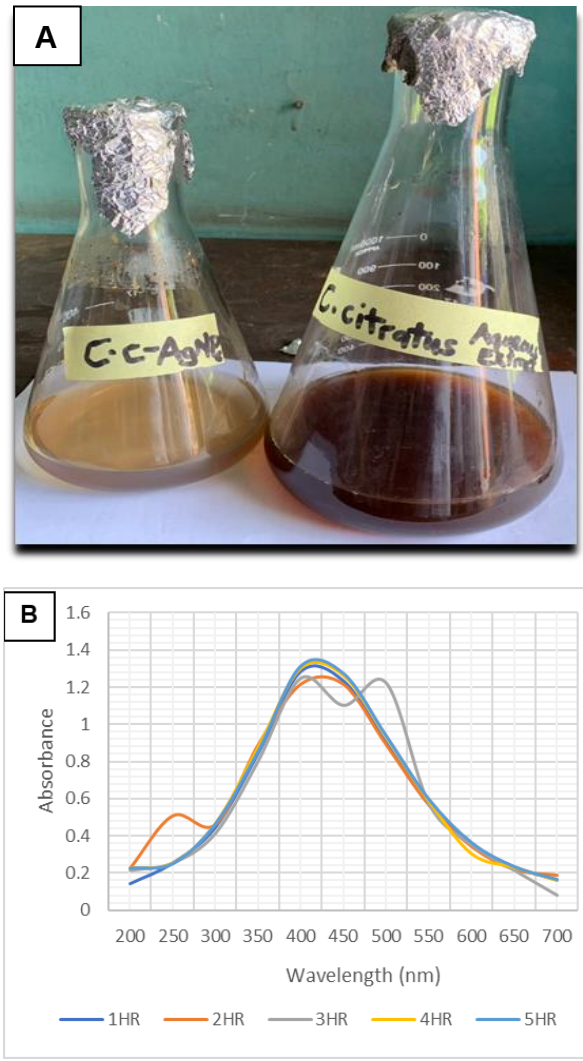

Figure 1: (a) Visual analysis of colour change **(b)** Absorbance readings (200-700 nm) observed in *Cymbopogon citratus* when silver nanoparticles were added. HR = Time (hours)

The FTIR result identified the major functional groups present in the synthesized AgNPs using *Cymbopogon citratus* aqueous leaf extract. The FTIR spectrum of the AgNPs showed a sharp absorbance between 1000 and 4000 cm^{-1}. The peak at 3265.1cm^{-1} indicates stretching of the O-H group of carboxylic acid, 2108.7 cm^{-1} indicates stretching of the C=C (alkyne) group, 1636.3 cm^{-1} indicates ethylene group (C=C) while 1025.0 cm^{-1} indicates stretching of C-O of alcohol group (Figure 3). These groups are capable of acting as reducing or capping agents. The XRD pattern of the synthesized AgNPs measured in the scan range of 10–70° showed a crystalline size on the X-ray diffractograms which supported the result of TEM in this study. The XRD spectrum confirmed the crystalline structure of the precipitate as silver (Ag). The XRD data for the synthesized AgNPs showed diffraction peaks at 2θ = 38°, 44.5° and 64.5° (Figure 4a and 4b), which can be indexed to the (111), (200), and (220) reflection planes, confirming the face-centered cubic crystalline structures of the nano-silver.[31,32]

ISSN 2616-0684 (Print)
ISSN 2616-0692 (Electronic)

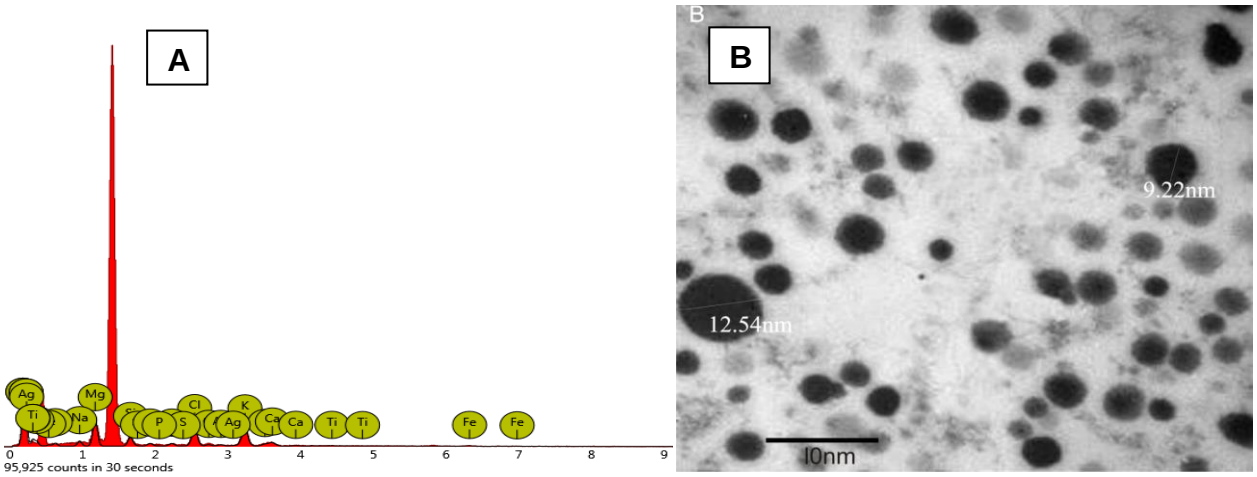

Figure 2: (a) Energy Dispersive X-ray and **(b)** Transmission electron microscope (TEM) Image of the synthesized *C. citratus* -AgNPs

The thermograph showed a weight loss which may be a function of the temperature from 30 to 950°C. CCALE is less stable than the conjugate (AgNPs) at temperatures less than 500°C (Figure 5), suggesting that AgNPs improved the stability below this temperature. However, AgNPs showed more stability than CCALE at all temperatures. The loss in weight could be due to the elimination of adsorbed water, oxidation of any remaining residual organics, and relaxation of the silica matrix as the temperature increases.[33] Table 1 shows the polyphenolic content of CCALE and its synthesized AgNPs. A statistically significant increase in total flavonoids, total phenolics, and total tannin content was observed in the synthesized AgNPs compared to the extract, indicating that silver nanoparticle synthesis may enhance the concentrations of polyphenolics in *Cymbopogon citratus* leaf. Such observation has been reported by Awote *et al.*[5, 22]

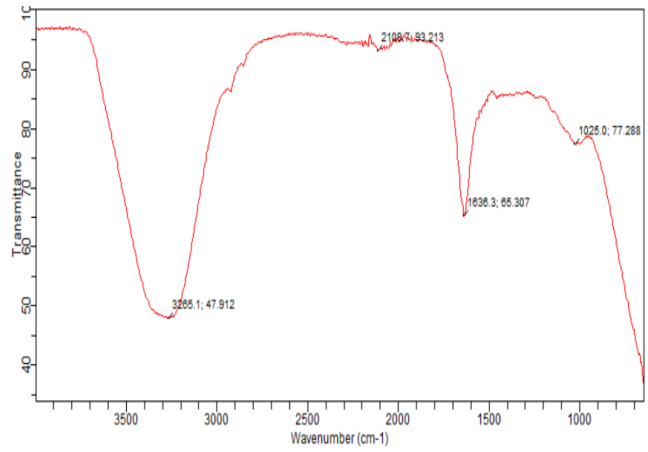

Figure 3: Fourier Transform Infra-red (FTIR) spectrum of the embedded functional groups in the synthesized AgNPs using CCALE

Table 2 and Figure 6 revealed the secondary metabolites present in *C. citratus* aqueous leaf extract using the GC-MS technique following the retention time, thirty-one (30) different compounds were found in this extract and all the thirty (30) compounds obeyed the Lipinski rule of five (RO5). Antioxidant properties have been thoroughly investigated and their ability to fend off damage from free radicals has been validated.[34] In Table 3, the synthesized AgNPs showed a significantly higher (p<0.05) antioxidant property than the CCALE. Similar results have been reported by Chavan *et al.* [35], and Menon *et al.*[36]. As suggested by Bolignano*et al.*[37], at least three *in-vitro* antioxidant methods have been used to confirm the antioxidant potential of CCALE and its synthesized AgNPs in this study. The results of this study showed that, the antioxidant property of AgNPs> CCALE in all four antioxidant methods which may infer that, while CCALE was capable of eliminating free radicals, the synthesized AgNPs using CCALE may be superior at stopping further free radicals from being generated. Furthermore, it appears that the contained phytochemicals may be responsible for these antioxidant properties. Table 4 shows the zone of inhibitions of each bacterium after treatment with CCALE or CCALE-AgNPs.

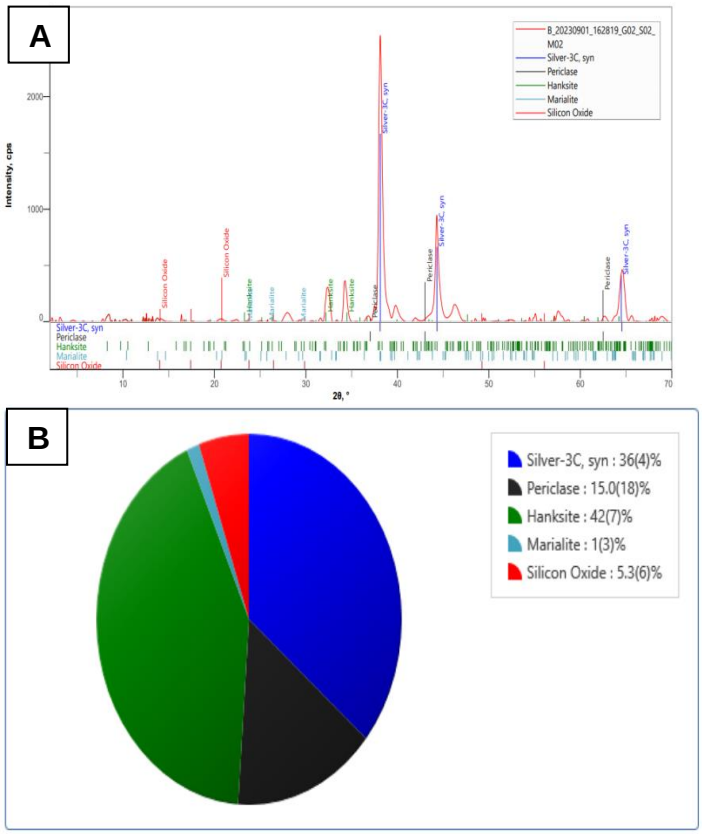

Figure 4: (a) X-ray diffraction (XRD) pattern and **(b)** Pie chart representation of the synthesized AgNPs using *C. citratus* aqueous leaf extract

Table 1: Polyphenolics contents of CCALE and its synthesized AgNPs

SAMPLES	TPC (mg/mL)	TFC (mg/mL)	TTC (mg/mL)
CCALE	49.21 ± 0.05[a]	96.94 ± 0.65[a]	27.44 ± 0.56[a]
CCALE-AgNPs	58.73 ± 0.21[b]	103.58 ± 0.33[b]	35.29 ± 0.35[b]

Results show Mean ± SEM of triplicate determinations and values with different alphabet in each column are significantly different from each other at $p< 0.05$.

Table 2: Compounds identified from the Gas-chromatography Mass Spectrometry (GC-MS) analysis of *Cymbopogon citratus* aqueous leaf extract

SN	Retention Time	Area %	Phytoconstituents	Lipinski rule
1.	7.636	2.34	Oxalic acid, cyclobutyltridecyl ester	Yes; 0 violation
			Decane, 1,1'-oxybis	Yes; 1 violation
			1-Dodecanol, 2-methyl-, (S)-	Yes; 0 violation
2.	12.203	3.20	Bicyclo[3.1.1]heptane, 2,6,6-tri...	Yes; 1 violation
			Neophytadiene	Yes; 1 violation
			1,7-Dimethyl-4-(propan-2-ylidene1,7-dimethyl-4-(propan-2-ylidene-11-oxabicyclo[8.1.0]undec-6-en-3-one	Yes; 0 violation
3.	12.569	2.68	6-Isopropenyl-4,8a-dimethyl-4a,5	Yes; 0 violation
			1-Hydroxypyrene	Yes; 0 violation
			6-Octen-1-ol, 3,7-dimethyl-, (R)-	Yes; 0 violation
4.	13.335	55.71	Dibutyl phthalate	Yes; 0 violation
			Phthalic acid, butyl 5-ethyl-1,3-dioxan-5-yl)methyl]benzene1,2-dicarboxylate,	Yes; 0 violation
			Phthalic acid, 5-methylhex-2-yl	Yes; 0violation
5.	13.496	4.10	Hexadecanoic acid, ethyl ester	Yes; 1 violation
			Ethyl 14-methyl-hexadecanoate	Yes; 1 violation
6.	14.863	6.32	Octadecanoic acid	Yes; 1 violation
			Oleic acid	Yes; 1 violation
			Pentadecanoic acid	Yes; 0 violation
7	17.225	6.48	Caparratriene	Yes; 1 violation
			Valerena-4,7(11)-diene (R)-2-((4aS,8aR)-4a-	Yes; 1 violation
			Methyl-8-methylene	Yes; 0 violation
8.	17.289	4.63	1,4-Dimethyl-8-isopropylidene tri	Yes; 1 violation
			Farnesyl bromide	Yes; 1 violation
9.	17.341	4.93	Lup-20(29)-en-3-one	Yes; 1 violation
			Aromandendrene	Yes; 1 violation
			1H-Cycloprop[e]azulene, decahydro	Yes; 1 violation
10.	18.462	7.31	1,4-benzene dicarboxylic acid	Yes; 0 violation
			Phthalic acid, monodecyl ester	Yes; 0 violation
			Phthalic acid, di(2-propyl pentyl	Yes; 1 violation
11.	20.442	2.32	Stigmasterol	Yes; 1 violation
			Cedran-diol	Yes; 0 violation

Table 3: Antioxidant potentials of CCALE and its synthesized AgNPs

Samples	FRAP (mg/g of AA)	TAC (%)	Reducing power (Absorbance)	DPPH (% Inhibition)
CCALE	0.866 ± 0.12[a]	51.96 ± 0.20[a]	0.970 ± 0.00[a]	83.2 ± 0.05[a]
CCALE-AgNPs	1.418 ± 0.05[b]	85.08 ± 0.60[b]	0.137 ± 0.03[b]	94.5 ± 0.01[b]

Results show Mean ± SEM of triplicate determinations and values with different alphabets are statistically different in each column at $p< 0.05$. FRAP: ferric reducing antioxidant power, TAC: total antioxidant capacity, DPPH: 2,2-diphenyl-1-picrylhydrazyl.

Treatment with CCALE-AgNPs showed a better zone of inhibition with resistance compared to CCALE which was resistant to four of the bacteria isolates including, *Proteus mirabilis*, *Escherichia coli*, *Pseudomonas aeruginosa* and *Staphylococcus aureus*. CCALE only inhibited two microorganisms, *Klebsiella pneumonia* and *Salmonella typhi*. However, treatment with CCALE-AgNPs inhibited all the selected bacteria isolates. This may indicate that the AgNPs possess a better antimicrobial activity against the selected bacterial isolates. *Proteus mirabilis* is a clinical microorganism found in the human urinary tract and it is well-known to cause urinary tract infection (UTI).

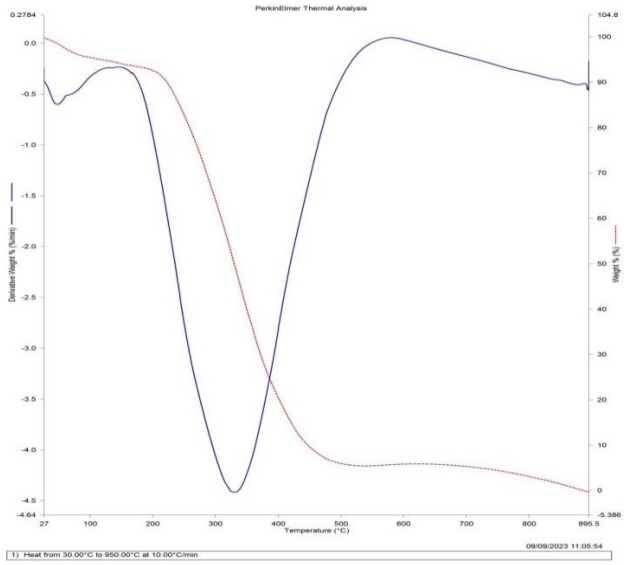

Figure 5: Thermograph from the Thermogravimetric Analysis (TGA) of *C. citratus* aqueous leaf extract and its synthesized AgNPs

Escherichia coli can be both a clinical and environmental microorganism, as many of the strains are part of the normal gut flora in humans and animals (clinical), however, the pathogenic strains can cause foodborne illnesses (environmental). *Pseudomonas aeruginosa* can also be a clinical and environmental microorganism. It is widely found in soil and water (environmental) and it is also a common cause of bloodstream infections and urinary tract infections (clinical). *Staphylococcus aureus* is commonly found on the skin and nose of healthy individuals but can cause minor skin infections, surgical site infections, bloodstream infections, and pneumonia. *Klebsiella pneumonia* is associated with pneumonia, bloodstream infections, and urinary tract infections (clinical). *Salmonella typhi* is the causative agent of typhoid fever (clinical), which is usually transmitted through contaminated food or water. The increased antibacterial activity of the synthesized AgNPs may be attributed to their large surface area which provides more surface contact with microorganisms.[38] Another important reason for the increased antibacterial activity of the AgNPs as a result of the clear zone of inhibition may be attributed to the synergistic effect between the phyto-components of CCALE and $AgNO_3$ that may cause a morphological alteration on the bacteria cell wall.[39] The mechanism of action of the antibacterial activity of AgNPs may result from respiratory chain and cell division attack which ultimately leads to cell death. Synthesized AgNPs have also been reported to release silver ions inside the bacterial cells, further enhancing their bactericidal activity.[40, 41]

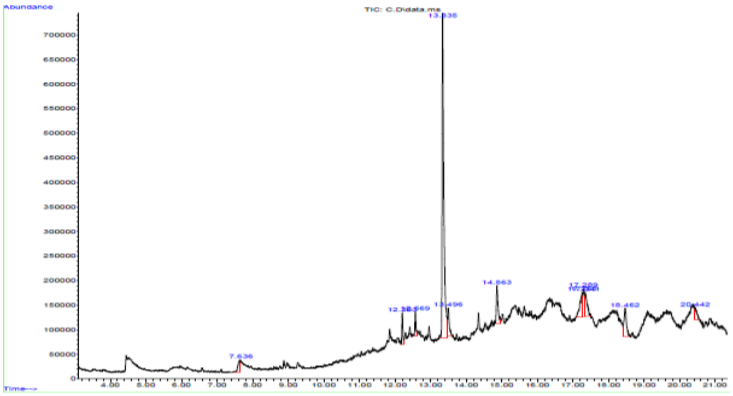

Figure 6: Chromatogram of secondary metabolites present in *Cymbopogon citrates* aqueous leaf extract

Figure 7 represents the 3D (left) and 2D (right) crystal structures of 11-*β*-hydroxysteroid dehydrogenase-stigmasterol interaction. Stigmasterol showed the best binding energy (-10.3 kcal/ mol) with the protein target with several interactions with the amino acids of the targeted proteins. Leu171, Ala172, Ser170, Gly216, Tyr183, Val227, Leu126, Val180, Leu215, Ile218, Val168, Asn119, His120, Thr220 and Gly47 of the protein target showed Vanderwaal interaction with the best binding ligand, stigmasterol. Conversely, Tyr177 showed pi-sigma interaction; Ile46, Val231, and Leu217 showed alkyl interaction; while Met223 and Ile121 showed pi-alkyl interaction. Table 5shows the order of the top five binding affinities of ligands docked with *11-β-hydroxysteroid* dehydrogenase. Stigmasterol showed the highest binding affinity with a binding energy of -10.3 Kcal/ mol, followed by 1H-cyclo(E)azulenedecahydro-1,1,4,7-tetramethyl (-9.2 Kcal/ mol), Lup-20(29)-e-3-one (-9.1 Kcal/mol), 1-hydroxy pyrene (-8.4 Kcal/mol), and 1,7-dimethyl-4-(propan-2-ylidene-11-oxabicyclo[8.1.0]undec-6-en-3-one (-8.1 Kcal/mol). Meanwhile, carbenoxolone (-6.6 Kcal/mol, position 7), a known standard drug and inhibitor of 11β-hydroxysteroid dehydrogenase was not among the top five ligands with good binding energy or binding affinity for 11β-hydroxysteroid dehydrogenase. Figure 8 shows the 3D (left) and 2D (right) crystal structures of the vaspin-sigmasterol complex. Stigmasterol showed the highest binding energy and hence, the best binding affinity with vaspin. Asp379, Asn191, Lys355, Glu194, Gln176, Lys414, Gln183, Gln176, Thr316, Thr314, and Phe139 are the core amino acids of the target protein that formed van der Waal interaction with stigmasterol. Meanwhile, Lys175 and Phe10 formed a pi-alkyl interaction, and Ile363 formed an alkyl interaction with stigmasterol. The 2D protein-ligand crystal structures showed various interactions/ bonds formed between the amino acids of the target proteins (11-*β*-hydroxysteroid dehydrogenase and vaspin) and the best binding ligand, stigmasterol. Each of these bonds may be responsible for the stability of the protein-ligand complex. The amino acid residues of 11-*β*-hydroxysteroiddehydrogenase and vaspin that interacted with stigmasterol play different biochemical functions.

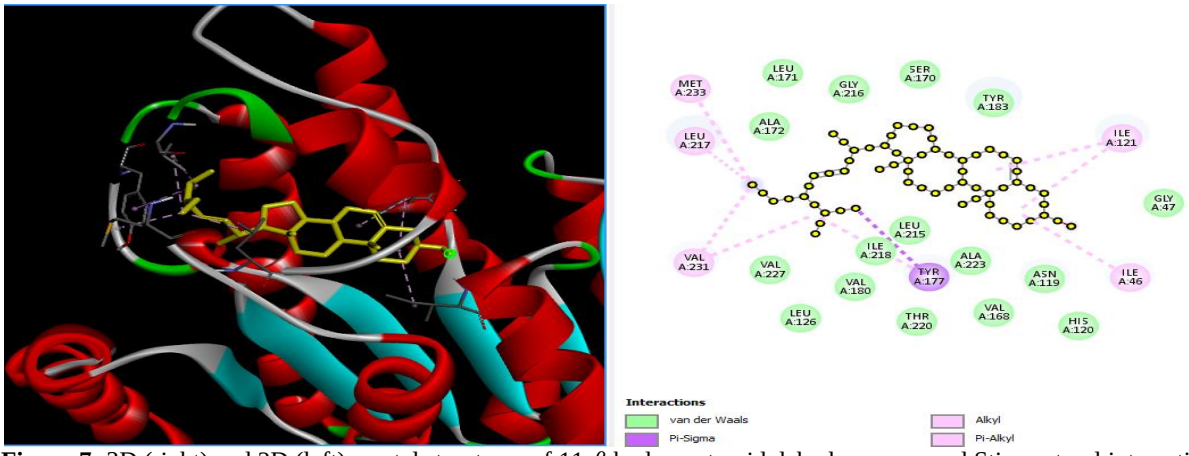

Figure 7: 3D (right) and 2D (left) crystal structures of 11-*β*-hydroxysteroid dehydrogenase and Stigmasterol interaction

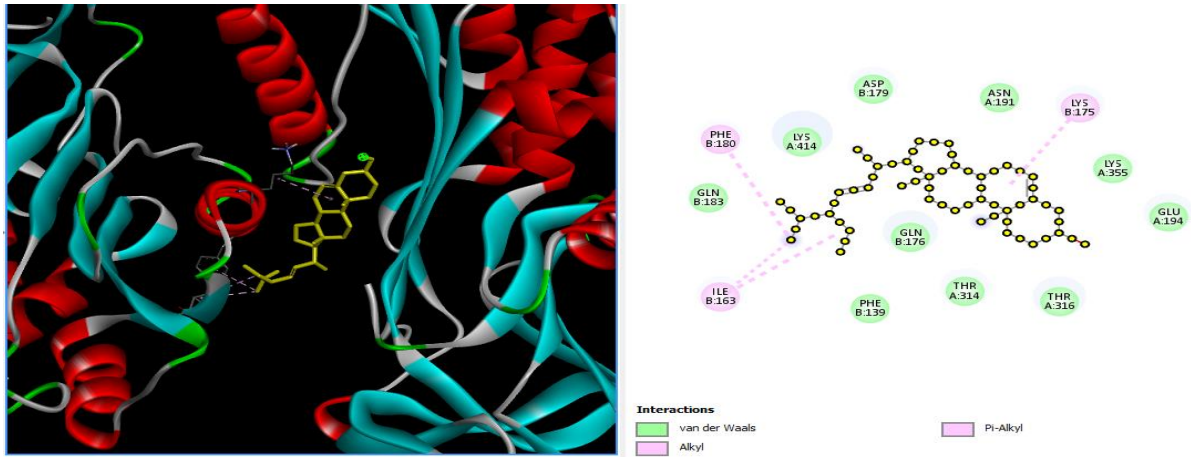

Figure 8: 3D (left) and 2D (right) crystal structures of Vaspin and stigmasterol interaction

Aspartate and glutamate participate in coordinating metal ions such as magnesium, zinc, and calcium while, asparagine and glutamine may form hydrogen bonds with the substrate, aiding substrate binding. Histidine plays a role in substrate binding and catalysis, thus acting as a general acid/base. Tyrosine participates in hydrogen bonding and substrate stabilization. Serine is often involved in catalytic mechanisms, potentially acting as a nucleophile to attack the substrate. Threonine is similar to serine by also acting as a nucleophile.[23]

Table 6shows the order of the top five binding affinities of ligands docked with vaspin. Stigmasterol showed the highest binding affinity with a binding energy of -8.8 Kcal/ mol, followed by Lup-20(29)-e-3-one (-8.6 Kcal/mol), 1H-cycloprop[e]azulene, decahydro-1,1,4,7-tetramethyl (-8.3 Kcal/ mol), 1-hydroxy pyrene (-7.5 Kcal/mol), and 1,7-dimethyl-4-(propan-2-ylidene-11-oxabicyclo[8.1.0]undec-6-en-3-one (-7.1 Kcal/mol). The synergy between computation and experimentation provides a comprehensive and intricate understanding of the mechanisms of action of synthesized silver nanoparticles. Since diabetes is still without a cure, the molecular docking technique has become an important player in drug discovery and development as it allows the prediction, viability, and interaction of drug candidates against a target protein,[42] including diabetes protein targets. ADMET properties are very imperative to predict the therapeutic potential of a candidate drug in living organisms.[43]

The ADMET properties of the top five ligands are predicted and described in Table 7.1–7.5. These properties include physicochemical, lipophilicity, water solubility, pharmacokinetics, drug-likeness, medicinal chemistry, and toxicity. The top five ligands obeyed the Lipinski rule of five (RO5),[44]which states that a molecule is more likely to be druggable if it has no more than five violations of the following criteria: molecular weight less than 500, log P less than 5, hydrogen bond donors less than 5, hydrogen bond acceptors less than 10, and 10 or fewer rotatable bond (Table 7.1). The low molecular weight of these compounds which is <500 g/mol may be the reason for the high binding affinities. Table 7.2 illustrates both water solubility and lipophilicity properties of the top five ligands. Log S (logarithm of solubility) is directly related to the water solubility of a drug, and it provides valuable information about a drug's solubility, which is crucial for understanding its absorption and distribution characteristics.

Table 4: Zone of Antibacterial Activity (nm)

Clinical Pathogens	CCALE	CCALE-AgNPs
Proteus mirabilis	0	17
Escherichia coli	0	17
Klebsiella pneumonia	20	20
Salmonella typhi	18	20
Pseudomonas aeruginosa	0	16
Staphylococcus aureus	0	20

CCALE: *Cymbopogon citratus* aqueous leaf extract, CCALE-AgNPs: *Cymbopogon citratus* aqueous leaf extract-synthesized silver nanoparticles.

ISSN 2616-0684 (Print)
ISSN 2616-0692 (Electronic)

Table 5: Binding affinities of top five ligands with 11-*β*-hydroxysteroid dehydrogenase

S/N	Ligands	PubChem ID	Binding Affinity (Kcal/ mol)
1.	Stigmasterol	5280794	-10.3
2.	1H-cyclo(E)azulene decahydro1,1,4,7-tetramethyl	520381	-9.2
3.	Lup-20(29)-e-3-one	92158	-9.1
4.	1-hydroxypyrene	21387	-8.4
5.	1,7-dimethyl-4-(propan-2-ylidene-11-oxabicyclo[8.1.0]undec-6-en-3-one	71438104	-8.1
	*Carbenoxolone	636403	-6.6

* Standard drug incorporated in this study for 11-*β*-hydroxysteroid dehydrogenase

Table 6: Binding affinities of top five ligands with vaspin

S/N	Ligands	PubChem ID	Binding Affinity (Kcal/ mol)
1.	Stigmasterol	5280794	-8.8
2.	Lup-20(29)-e-3-one	92158	-8.6
3.	1H-cycloprop[e]azulene, decahydro-1,1,4,7-tetramethyl	520381	-8.3
4.	1-hydroxypyrene	21387	-7.5
5.	1,7-dimethyl-4-(propan-2-ylidene-11-oxabicyclo[8.1.0]undec-6-en-3-one	71438104	-7.1

Table 7.1: Predicted physiochemical properties of top five ligands

SN	Ligands	Molecular Formula	Molecular weight (g/mol)	No. rotatable bonds	No. H-bond acceptors	No. H-bond donors
1.	Stigmasterol	$C_{29}H_{48}O$	412.69	5	1	1
2.	1H-cycloprop[e]azulene, decahydro-1,1,4,7-tetramethyl-	$C_{15}H_{26}$	206.37	0	0	0
3.	Lup-20(29)-e-3-one	$C_{30}H_{48}O$	424.70	1	1	0
4.	1-hydroxypyrene	$C_{16}H_{10}O$	218.25	0	1	1
5.	1,7-dimethyl-4-(propan-2-ylidene-11-oxabicyclo [8.1.0]undec-6-en-3-one	$C_{15}H_{22}O_2$	234.33	0	2	0

Table 7.2: Predicted water solubility and Lipophilicity of top five ligands

SN	Ligands	Water solubility Log S (ESOL)	Class	Lipophilicity Log Po/w (iLOGP)
1.	Stigmasterol	-7.46	Poorly soluble	5.08
2.	1H-cycloprop[e]azulene, decahydro-1,1,4,7-tetramethyl-	-4.60	Moderately soluble	3.35
3.	Lup-20(29)-e-3-one	-8.43	Poorly soluble	4.54
4.	1-hydroxypyrene	-4.81	Moderately soluble	2.06
5.	1,7-dimethyl-4-(propan-2-ylidene-11-oxabicyclo [8.1.0]undec-6-en-3-one	-3.05	Soluble	2.87

Stigmasterol and Lup-20(29)-e-3-one are poorly soluble, 1H-Cycloprop[e]azulene,decahydro-1,1,4,7-tetramethyl- and 1-hydroxypyrene are moderately soluble while, 1,7-dimethyl-4-(propan-2-ylidene-11-oxabicyclo[8.1.0]undec-6-en-3-one is soluble in water. Stigmasterol showed the best logarithm of the partition coefficient (Log P) with a value of 5.08. Additionally, other ligands were also predicted to be within the ranges away from zero (0) indicating their good lipophilicity properties in drug discovery. The assessment of water solubility properties showed that the compound with the best binding affinity, stigmasterol, is poorly soluble but highly lipophilic. Stigmasterol lipophilicity property may indicate a better transversion of the drug through the lipid bilayer for better metabolism.[23]Moreso, the compound may easily diffuse and be transported across the biological membrane.[45]The top five ligands showed positive pan-assay interference compounds (PAINS) and lead-likeness indications, which may indicate that these compounds are not likely to give false positive results in high throughput screens. These ligands also revealed the synthetic accessibility score to be between the range of 1.0 – 6.21, where the ligand with the best energy and affinity to the targeted proteins showed better feasibility to be synthesized. Additionally, each of these ligands showed a good bio-availability score of 0.55 which is a good drug-likeness property since a minimum of 0.10 bioavailability score is required of a compound to be considered as a drug candidate (Table 7.3). Table 7.4 shows the pharmacokinetics of the top five active compounds embedded in *Cymbopogon citratus* leaf. Stigmasterol, 1H-cycloprop[e]azulene, decahedron-1,1,4,7-tetramethyl-, and lup-20(29)-e-3-one are the three of the top five ligands that showed low gastrointestinal absorption and negative blood-brain barrier (BBB) indication while, 1-hydroxypyrene and 1,7-dimethyl-4-(propan-2-ylidene-11-oxabicyclo[8.1.0]undec-6-en-3-one showed high gastrointestinal absorption and positive indication for blood-brain barrier permeability.

Table 7.3: Medicinal Chemistry and Drug-likeness of top five ligands

SN	Ligands	PAINS	Lead-likeness	Synthetic accessibility	Bioavailability Score
1.	Stigmasterol	0 alert	No	6.21	0.55
2.	1H-cyclo(E)azulene, decahydro-1,1,4,7-tetramethyl	0 alert	No	3.78	0.55
3.	Lup-20(29)-e-3-one	0 alert	No	5.38	0.55
4.	1-hydroxypyrene	0 alert	No	1.00	0.55
5.	1,7-dimethyl-4-(propan-2-ylidene-11-oxabicyclo [8.1.0]undec-6-en-3-one	0 alert	No	4.31	0.55

Table 7.4: Pharmacokinetics prediction

SN	Ligands	GI absorption	BBB permeant	P-gp substrate	CYP1A2 inhibitor	CYP2C19 inhibitor	CYP2C9 inhibitor	CYP2D6 inhibitor	CYP3A4 inhibitor
1.	Stigmasterol	Low	No	No	No	No	Yes	No	No
2.	1H-Cycloprop[e] azulen, decahydro-1,1,4,7-tetramethyl-	Low	No	No	Yes	Yes	Yes	No	No
3.	Lup-20(29)-e-3-one	Low	No	No	No	No	No	No	No
4.	1-hydroxypyrene	High	Yes	No	Yes	Yes	No	No	No
5.	1,7-dimethyl-4-(propan-2-ylidene-11-oxabicyclo [8.1.0]undec-6-en-3-one	High	Yes	No	No	No	No	No	No

These two compounds, 1-hydroxy pyrene and 1,7-dimethyl-4-(propan-2-ylidene-11-oxabicyclo[8.1.0]undec-6-en-3-one, may be developed for use in the treatment of central nervous system (CNS) disorders, especially neurological disorders including Alzheimer's disease (AD), schizophrenia, dementia, etc. None of these top five ligands were identified as a P-glycoprotein substrate. P-glycoproteins are transmembrane efflux pumps that function to pump out substrates such as drugs out of the cell.[46] This may infer that the candidate drugs may have high cellular absorption into compartments. Also, none of these top five ligands was predicted to be CYP2D6 and CYP3A4 inhibitors. However, 1H-cycloprop[e]azulene,decahydro-1,1,4,7-tetramethyl-, and 1-hydroxypyrene were identified as the only inhibitors of CYP1A2 and CYP2C19. Conversely, Stigmasterol and 1H-cycloprop[e]azulene, decahydro-1,1,4,7-tetramethyl-, were predicted as CYP2C9 inhibitors.

PPAR-γ plays a vital role in glucose and lipid metabolism, adipogenesis, and inflammation regulation, all of which are critical diabetic conditions. Its activation improves insulin sensitivity and glycemic control, making it a valuable target for diabetes treatment. Conversely, the Nrf2/ARE pathway also plays a crucial role in combating oxidative stress, a key factor in the development and progression of diabetes. The activation of this pathway enhances antioxidant defenses, improves insulin sensitivity, protects pancreatic beta cells, and mitigates the complications associated with diabetes. [47] Targeting these pathways is promising for the development of new therapeutic strategies in managing diabetes and its complications. The

top five ligands in this study were predicted to be inactive in these pathways. 1,7-dimethyl-4-(propan-2-ylidene-11-oxabicyclo[8.1.0]undec-6-en-3-one that predicted a positive indicator for the liver may call for this compound in preclinical and clinical trials (Table 7.5). Table 7.5 illustrates the prediction of the top five active compounds embedded in *Cymbopogon citrates* aqueous leaf extract. All the ligands predicted a negative indicator for both the liver and kidney except for 1,7-dimethyl-4-(propan-2-ylidene-11-oxabicyclo[8.1.0]undec-6-en-3-one which predicted a positive indicator for the liver. Further prediction also showed that all the top five ligands cannot result in carcinogenicity, immunogenicity, mutagenicity, and cytotoxicity. Additionally, these ligands are predicted to be inactive against Peroxisome Proliferator-activated receptor gamma (PPAR-γ); Nuclear factor (erythroid-derived 2)-like 2/antioxidant responsive element (nrf2/ARE); Heat shock factor response element (HSE).[48]

Table 7.5: Predicted Toxicity of top five ligands

SN	Ligands	Hepato-toxicity	Carcino-genicity	Immuno-toxicity	Muta-genicity	Cyto-toxicity	PPAR-δ	nrf2/ARE
1.	Stigmasterol	Inactive	Inactive	Inactive	Inactive	Inactive	Inactive	Inactive
2.	1H-Cycloprop[e]azulene, decahydro-1,1,4,7-tetramethyl-	Inactive	Inactive	Inactive	Inactive	Inactive	Inactive	Inactive
3.	Lup-20(29)-e-3-one	Inactive	Inactive	Inactive	Inactive	Inactive	Inactive	Inactive
4.	1-hydroxypyrene	Inactive	Inactive	Active	Inactive	Inactive	Inactive	Inactive
5.	1,7-dimethyl-4-(propan-2-ylidene-11-oxabicyclo [8.1.0]undec-6-en-3-one	Active	Inactive	Inactive	Inactive	Inactive	Inactive	Inactive

Peroxisome Proliferator-Activated Receptor Gamma (PPAR-γ); Nuclear factor (erythroid-derived 2)-like 2/antioxidant responsive element (nrf2/ARE)

Conclusion

The results of this study support the use of *Cymbopogon citratus* aqueous leaf extract (CCALE) for the synthesis of silver nanoparticles (AgNPs), and the synthesized AgNPs showed promising antioxidant and antibacterial properties *in vitro*. Furthermore, the secondary metabolites of CCALE, especially stigmasterol predicted antidiabetic potential *in-silico*, which may be considered a drug candidate in treating diabetes mellitus and its related complications. These biological activities observed in this study may be attributed to *Cymbopogon citratus* polyphenolic phytoconstituents. However, there's a need to validate these findings *in vivo* using animal models such as experimental rats and *Drosophila melanogaster*.

Conflict of Interest

The authors declare no conflict of interest.

Author's Declaration

The authors hereby declare that the work presented in this article is original and that any liability for claims relating to the content of this article will be borne by them.

Acknowledgments

The authors are grateful to the Department of Biochemistry, the Department of Microbiology, and the Department of Botany, Lagos State University, Ojo, Nigeria, for providing the research facilities.

References

1. Omran BA and Omran BA. Fundamentals of nanotechnology and nanobiotechnology. Nanobiotechnology: A Multidisciplinary Field of Science. Springer. 2020; 6:1-36p.
2. Behravan M, Panahi AH, Naghizadeh A, Ziaee M, Mahdavi R, Mirzapour A. Facile green synthesis of silver nanoparticles using *Berberis vulgaris* leaf and root aqueous extract and its antibacterial activity. Int J Biol Macromol. 2019; 124: 148-154.
3. Sajid M and Płotka-Wasylka J. Nanoparticles: Synthesis, characteristics, and applications in analytical and other sciences. Microchem J. 2020; 154: 104623.
4. Teodoro KBR, Migliorini FL, Facure MHM, Sanfelice RC, Martins D, Correa DS. Novel Chemical Sensors Based on Green Composite Materials for Environmental Analysis. Nanosensors Environ. Food Agric. 2021; 1: 109-138.
5. Awote OK, Kazeem MI, Ojekale AB, Ayanleye OB, Ramoni HT. Prospects of silver nanoparticles (AgNPs) synthesized by *Justicia secunda* aqueous extracts on diabetes and its related complications. Proc Nig Acad Sci. 2023a; 16(1): 87-105.
6. Thakur S, Sharma S, Thakur S, Rai R. Green synthesis of copper nanoparticles using *Asparagus adscendens* roxb. Root and leaf extract and their antimicrobial activities. Int J Curr Microbiol Appl Sci. 2018; 7(4): 683-694.
7. Christensen L, Vivekanandhan S, Misra M, Kumar Mohanty A. Biosynthesis of silver nanoparticles using *Murraya koenigii* (curry leaf): an investigation on the effect of broth concentration in reduction mechanism and particle size. Adv. Mater. 2011; 2(6): 429-434.
8. Wypij M, Jędrzejewski T, Trzcińska-Wencel J, Ostrowski M, Rai M. Golińska P. Green synthesized silver nanoparticles: antibacterial and anticancer activities, biocompatibility, and analyses of surface-attached proteins. Front Microbiol. 2021; 12: 632505.
9. Najmi A, Javed SA, Al Bratty M, Alhazmi HA. Modern approaches in the discovery and development of plant-based natural products and their analogs as potential therapeutic agents. Molecules. 2022; 27(2):349.
10. Laldingliani T, Thangjam NM, Zomuanawma R, Bawitlung L, Pal A and Kumar A. Ethnomedicinal study of medicinal plants used by Mizo tribes in the Champhai district of Mizoram, India. J Ethnobiol Ethnomed. 2022; 18(1): 1-29.
11. Unuofin JO and Lebelo SL. Antioxidant effects and mechanisms of medicinal plants and their bioactive compounds for the

prevention and treatment of type 2 diabetes: an updated review. Oxid Med Cell Longev. 2020; 2020:1356893.
12. Okaiyeto K and Oguntibeju OO. African herbal medicines: Adverse effects and cytotoxic potentials with different therapeutic applications. Int. J. Environ. Public Health. 2021; 18(11):5988.
13. Sahal G, Woerdenbag HJ, Hinrichs WL, Visser A, Tepper PG, Quax WJ, van der Mei HC, Bilkay IS. Antifungal and biofilm inhibitory effect of *Cymbopogon citratus* (lemon grass) essential oil on biofilm forming by *Candida tropicalis* isolates; an in vitro study. J Ethnopharmacol. 2020; 246: 112188.
14. Sen S, Israr M, Singh S, Singh MK, Verma RS, Bawankule DU. Pharmaceutical, cosmeceutical, food additive and agricultural perspectives of *Cymbopogon martini*: A potential industrial aromatic crop. S Afr J Bot. 2023; 158: 277-291.
15. Jamshidi-Kia F, Wibowo J P, Elachouri M. The battle between plants as antioxidants with free radicals in the human body. J Herb Med Pharmacol. 2020; 9(3): 191-199.
16. Mukarram M, Choudhary S, Khan MA, Poltronieri P, Khan MMA, Ali J, Kurjak D, Shahid M. Lemongrass essential oil components with antimicrobial and anticancer activities. Antioxidants. 2021; 11(1): 20.
17. Dewanti NPN, Pertiwi AD, Utami EF, Idawati S, Suhada A, Mazlan NAA, Purmafitriah E. Antidiabetic Effect Test of Combination of Ginger (*Zingiber officinale*), Lemongrass (*Cymbopogon citratus*), and Cinnamon (*Cinnamomum verum*) on Male Mice (*Mus musculus*). Proc Int Conf Med Technol. 2022; 51: 62.
18. Kiani HS, Ali A, Zahra S, Hassan ZU, Kubra KT, Azam M, Zahid HF. Phytochemical composition and pharmacological potential of lemongrass (*Cymbopogon*) and impact on gut microbiota. Appl Chem. 2022; 2(4): 229-246.
19. Lin MC, Liu CC, Lin YC, Liao CS. Resveratrol protects against cerebral ischemic injury via restraining lipid peroxidation, transition elements, and toxic metal levels, but enhancing anti-oxidant activity. Antioxidants. 2021; 10(10): 1515.
20. Loko YLE, MedeganFagla S, Kassa P, Ahouansou CA, Toffa J, Glinma B, Dougnon V, Koukoui O, Djogbenou SL, Tamò M, Gbaguidi F. Bioactivity of essential oils of *Cymbopogon citratus* (DC) Stapf and *Cymbopogonn ardus* (L.) W. Watson from Benin against *Dinoderus porcellus lesne* (Coleoptera: Bostrichidae) infesting yam chips. Int J Trop Insect Sci. 2021; 41: 511-524.
21. Fatunmibi OO, Njoku IS, Asekun OT, Ogah JO. Chemical composition, antioxidant and antimicrobial activity of the essential oil from the leaves of *Cymbopogon citratus* . Am J Essent Oil. 2023; 11(1): 01-05.
22. Awote OK, Adeyemo AG, Apete SK, Awosemo RB, Azeez HD, Salako DS, Kayode BD, Arowolo SO, Olatubosun OS, Olalero FE. *Jatropha tanjorensis* aqueous extracts synthesized silver nanoparticles possess antidiabetic, antiglycation, antioxidant, and anti-inflammatory potentials. J Res Rev Sci. 2023b; 10: 41-55.
23. Awote OK, Kanmodi RI, Ebube SC, Abdulganniyyu ZF. Nutritional Profile, GC-MS Analysis and *In-silico* Anti-diabetic Phytocompounds Candidature of *Jatropha gossypifolia* Leaf Extracts. Curr Drug Discov Technol. 2024; 21(3): 32-45.
24. Bhatia D, Mittal A, Malik DK. Antimicrobial potential and in vitro cytotoxicity study of polyvinyl pyrollidone-stabilized silver nanoparticles synthesized from *Lysinibacillus boronitolerans*. IET Nanobiotechnol. 2021; 15(4): 427-440.
25. Bano N, Iqbal D, Al Othaim A, Kamal M, Albadrani HM, Algehainy NA, Alyenbaawi H, Alghofaili F, Amir M, Roohi R. Antibacterial efficacy of synthesized silver nanoparticles of *Microbacterium proteolyticum* LA2 (R) and *Streptomyces rochei* LA2 (O) against biofilm forming meningitis causing microbes. Sci Rep. 2023; 13(1): 4150.
26. Majeed S, Saravanan M, Danish M, Zakariya NA, Ibrahim MNM, Rizvi EH, un NisaAndrabi S, Barabadi H, Mohanta, Y.K., Mostafavi, E. Bioengineering of green-synthesized TAT peptide-functionalized silver nanoparticles for apoptotic cell-death mediated therapy of breast adenocarcinoma. Talanta. 2023; 253: 124026.
27. Sun L, Zhang Z, Dang H. A novel method for preparation of silver nanoparticles. Mater. Lett. 2003; 57(24-25): 3874-3879.
28. Awote OK, Anagun OS, Adeyemo AG, Igbalaye JO, Ogun ML, Apete SK, Folami SO, Olalero FE, Ebube SC, Taofeeq MI. Akinloye OO. Green-synthesized silver nanoparticles by using fresh *Justicia Secunda*, *Telfairia occidentalis*, and *Jatropha tanjorensis* aqueous leaf extracts against clinical and environmental bacterial isolates. Asian J Green Chm. 2022: 6(4): 284-296.
29. Rakib-Uz-Zaman SM, HoqueApu E, Muntasir MN, Mowna SA, Khanom MG, Jahan SS, Akter NR, Khan MA, Shuborna NS, Shams SM, Khan K. Biosynthesis of silver nanoparticles from *Cymbopogon citratus* leaf extract and evaluation of their antimicrobial properties. Challenges. 2022; 13(1):18.
30. Odeyemi SW, Ajayi EO, Otunola GA, Afolayan AJ. Silver nanoparticles biosynthesis by *Elaeodendron croceum* Stem bark and leaves extracts, their anti-bacterial and cytotoxicity activities. Inorg Nano-Met Chem. 2020; 51(3):399-410.
31. Norashikin A. Preparation of electrospun polyvinylidene fluoride/nanosilver nanofibrous membrane and its antimicrobial potential/Norasikin Ahmad (Doctoral dissertation, University of Malaya). 2018.
32. Abdul Aziz NS, Isa N, Osman MS, Wan Kamis WZ, So'aib MS, MohdAriff MA. A Mini Review on the Effects of Synthesis Conditions of Bimetallic Ag/Si Nanoparticles on Their Physicochemical Properties. Int J Nanosci Nanotechnol. 2023; 18(4): 219-232.
33. Wang J, Jia G, Kong H, Li H, Zuo R, Yang Y, Zhang C. Highly efficient luminescence and enhanced stability of nanocomposites by encapsulating perovskite quantum dots in defect-related luminescent silica nanospheres. Appl Surf Sci. 2022; 591: 153258.
34. Awote OK, Adeyemo AG, Igbalaye JO, Awosemo RB, Ibrahim AB, Abdulrafiu F, Fajobi T. In Vitro Alpha-Amylase Inhibitory Activity, Antioxidant Activity and HPLC Analysis of *Eichhornia crassipes* (water hyacinth) Methanol Extracts. Trop J Nat Prod Res. 2021; 5(12):2174-2181.
35. Chavan C, Mulik S, Chavan M, Adnaik R, Patil P. Screening of antioxidant activity and phenolic content of whole plant of *Barleria prionitis* Linn. Int J Res Ayurv Pharm. 2011; 2(4): 1313-1319.
36. Menon S, Agarwal H, Kumar SR, Kumar SV. Green synthesis of silver nanoparticles using medicinal plant *Acalypha indica* leaf extracts and its application as an antioxidant and antimicrobial agent against foodborne pathogens. Int J Appl Pharm. 2017; 9(5): 42-50.
37. Bolignano D, Cernaro V, Gembillo G, Baggetta R, Buemi M, D'Arrigo G. Antioxidant agents for delaying diabetic kidney disease progression: A systematic review and meta-analysis. PloS One. 2017; 12(6): e0178699.
38. Logeswari P, Silambarasan S, Abraham J. Synthesis of silver nanoparticles using plant extract and analysis of their antimicrobial property. J Saudi Chem Soc. 2015; 19(3): 311-317.
39. Durán N, Durán M, De Jesus MB, Seabra AB, Fávaro WJ, Nakazato G. Silver nanoparticles: A new view on mechanistic aspects of antimicrobial activity. Nanomed: Nanotechnol Biol Med. 2016; 12(3): 789-799.
40. Morones JR, Elechiguerra JL, Camacho A, Holt K, Kouri JB, Ramírez JT, Yacaman MJ. The bactericidal effect of silver nanoparticles. Nanotechnol. 2005; 16(10): 2346.
41. Panáček A, Kvítek L, Smékalová M, Večeřová R, Kolář M, Röderová M, Dyčka F, Šebela M, Prucek R, Tomanec O, Zbořil R. Bacterial resistance to silver nanoparticles and how to overcome it. Nat nanotechnol. 2018; 13(1), 65-71.
42. Riyaphan J, Pham DC, Leong MK, Weng CF. *In silico* approaches to identify polyphenol compounds as α-glucosidase and α-

amylase inhibitors against type-II diabetes. Biomol. 2021; 1(12): 1877.

43. Wu C, Liu Y, Yang Y, Zhang P, Zhong W, Wang Y, Wang Q, Xu Y, Li M, Li X, Zheng M. Analysis of therapeutic targets for SARS-CoV-2 and discovery of potential drugs by computational methods. Acta Pharm Sin B. 2020; 10:766-788.
44. Lipinski CA. Lead-and drug-like compounds: the rule-of-five revolution. Drug Discov. Today Technol. 2004; 1(4): 337-341.
45. Sharma AD and Kaur I. Essential oil from *Cymbopogon citratus* exhibits "anti-aspergillosis" potential: *in-silico* molecular docking and *in vitro* studies. Bull Natl Res Cent. 2022; 46(1):23.
46. Sharom FJ. Complex interplay between the P-glycoprotein multidrug efflux pump and the membrane: its role in modulating protein function. Front Oncol. 2014; 3(4):41.
47. Awote OK, Apete SK, Igbalaye JO, Adeyemo AG, Dele-osedele PI, Thomas-Akinwale K, Boniwey TS, Ogunbamowo AA, Ebube SC, Folami SO. Phytochemical Screening, Antioxidant, and α-Amylase Inhibitory Activities of *Acacia nilotica* Seed Methanol Extract. Adv J Curr Res. 2022; 7(8): 1-27.
48. Gulwe AB, Ebube SC, Awote OK, Ambhore AN. Molecular Docking Study of Selected Bioactive Compounds in Alzheimer's Disease using BACE-1 (PDB ID: 5QCU) as Target Protein. J Popul Ther Clin Pharmacol. 2023; 30(3): 787-793.